
**Liquid Crystals**
Publication details, including instructions for authors and subscription information:
http://www.informaworld.com/smpp/title~content=t713926090

# Azimuthal director gliding at a strongly anchoring interface of polyimide

Sandro Faetti[a]; Prisca Marianelli[a]
[a] INFM and Dipartimento di Fisica di Pisa, 56127 Pisa, Italy

**To cite this Article** Faetti, Sandro and Marianelli, Prisca(2006) 'Azimuthal director gliding at a strongly anchoring interface of polyimide', Liquid Crystals, 33: 3, 327 — 334
**To link to this Article: DOI:** 10.1080/02678290500512227
**URL:** http://dx.doi.org/10.1080/02678290500512227

*Liquid Crystals*, Vol. 33, No. 3, March 2006, 327–334



# Azimuthal director gliding at a strongly anchoring interface of polyimide

SANDRO FAETTI* and PRISCA MARIANELLI
INFM and Dipartimento di Fisica di Pisa, Largo Pontecorvo 3, 56127 Pisa, Italy

(*Received 8 August 2005; accepted 2 November 2005*)

A gliding of the director at the interface between a nematic liquid crystal and a solid medium is generally observed at many interfaces giving weak or moderately strong anchoring. This phenomenon is characterized by strongly non-linear dynamics and very long relaxation times (hours–days). The gliding of the director has also been observed very recently at the interface between a rubbed polyimide layer and a nematic liquid crystal which gives strong azimuthal anchoring. However, due to the weak nature of the experimental signals that characterizes the strong anchoring, this latter measurement was appreciably affected by thermal drift. In this paper, we develop a new experimental reflectometric method whereby the thermal drift is appreciably reduced. The method allows us to obtain more accurate signals and to investigate their time dependence. It is shown that the director gliding is well represented by a stretched exponential, as well as in the case of weak anchoring substrates. These measurements confirm that the gliding of the director is a universal phenomenon characterizing any kind of substrate with either weak and strong anchoring.



## 1. Introduction

In the nematic liquid crystal (NLC) continuum theory [1], the average orientation of the molecules is denoted by the unit vector $\mathbf{n}(\mathbf{r})$ which is termed the director. The equilibrium configuration of the director-field is reached when the total free energy of the system is minimized and no torque acts on the director. The surface interactions are characterized by the anchoring energy $W(\mathbf{n}_s)$, which depends on the zenithal angle $\theta_s$ of the surface director $\mathbf{n}_s$ with respect to the normal to the interface, and on the azimuthal angle $\varphi_s$ with respect to an $x$-axis in the surface local plane. If only $\varphi_s$ is changed, the anchoring energy becomes a function $W(\varphi_s)$ of the azimuthal angle only, and is termed azimuthal anchoring energy. Experimental results [3, 4] show that the azimuthal anchoring energy $W(\varphi_s)$ is usually well represented by the Rapini–Papoular form [1, 2]:

$$W(\varphi_s) = \frac{W_a}{2}\sin^2(\varphi_s - \varphi_e) \qquad (1)$$

where $W_a$ is the anchoring energy coefficient and $\varphi_e$ is the azimuthal easy angle that corresponds to the orientation that minimizes the anchoring energy. The anchoring is strong if $W_a > 10^{-4}\,\mathrm{J\,m^{-2}}$, and weak if $W_a < 10^{-5}\,\mathrm{J\,m^{-2}}$. If an azimuthal electric external torque is applied, the director reorients everywhere as soon as a new equilibrium configuration is reached. In the case of a strong anchoring energy, the external torque is unable to change appreciably the surface director and, thus, $\varphi_s$ always remains close to $\varphi_e$. The azimuthal anchoring energy in equation (1) can then be suitably approximated with the parabolic form:

$$W(\varphi_s) = \frac{W_a}{2}(\varphi_s - \varphi_e)^2. \qquad (2)$$

Under these conditions ($\varphi_s \approx \varphi_e$), the equation which describes the time evolution of the surface director angle $\varphi_s$ at the incidence surface $z = z_1$ is:

$$K_{22}\left.\frac{\partial\varphi}{\partial z}\right|_{z=z_1} - W_a(\varphi_s - \varphi_e) = \xi_\gamma \frac{\partial\varphi_s}{\partial t} \qquad (3)$$

where $K_{22}$ is the twist elastic constant [1], $\xi_\gamma$ is the surface orientational viscosity [5] and $\left.\frac{\partial\varphi}{\partial z}\right|_{z=z_1}$ is the derivative of the director azimuthal angle at the interface. The first term in the left hand side of equation (3) is the azimuthal surface elastic torque, whilst the second term is the anchoring restoring torque.

In principle, the surface viscosity in equation (3) introduces a time delay $\tau_D = \xi_\gamma / W_a$ between the surface elastic torque and the consequent surface rotation $\varphi_s - \varphi_e$. However, according to a simple dimensional analysis, the surface orientational viscosity is $\xi_\gamma = \gamma L_{mol}$, where $\gamma$ is the bulk orientational viscosity [1] and $L_{mol}$ is

*Corresponding author. Email: Faetti@df.unipi.it

*Liquid Crystals*
ISSN 0267-8292 print/ISSN 1366-5855 online © 2006 Taylor & Francis
http://www.tandf.co.uk/journals
DOI: 10.1080/02678290500512227

a characteristic length. In a recent experiment, Mertelj and Copic [5] found $L_{mol} \approx 10\,nm$. In our experiment, the anchoring energy coefficient at room temperature is $W_a \approx 0.4 \times 10^{-3}\,J\,m^{-2}$ and, thus, using the experimental values $\gamma = 0.077\,Pa\,s$ [6] and $L_{mol} \approx 10\,nm$, we find $\tau_D = \xi_\gamma / W_a \approx 2\,\mu s$. The bulk relaxation time at the switching on of the electric field $E$ is given by $\tau_{bulk} = \gamma/(\varepsilon_a\,\varepsilon_o\,E^2)$, where $\varepsilon_a$ is the anisotropy of the dielectric constant. Substituting in this expression the measured values $\gamma = 0.077\,Pa\,s$ [6] and $\varepsilon_a = 13.1$ [7] for 5CB at $T = 25^\circ C$, together with our maximum electric field $E = 0.3\,V\,\mu m^{-1}$, we find $\tau_{bulk} \approx 7\,ms$. This time is more than three orders of magnitude higher then the surface delay time $\tau_D$ in our experiment. Therefore, the viscosity term in equation (3) can be completely disregarded and the surface director angle follows the surface elastic torque. The surface director angle should reach a constant equilibrium value after a few characteristic times $\tau_{bulk}$.

However, there are many experimental observations on weak or moderately strong anchoring demonstrating that the actual surface behaviour is much more complex [3, 4, 8–14]. In particular, two very different dynamic regimes are always observed. A detailed investigation of these two regimes was reported [14] in which the surface dynamics at the interface between the liquid crystal 5CB and an obliquely evaporated SiO thin layer was investigated. A special optical method was used to measure simultaneously the surface elastic torque ($\Gamma_e = K_{22} \left.\frac{\partial \varphi}{\partial z}\right|_{z=z_1}$) and the director surface angle $\varphi_s$ after the switching on of a magnetic field. In accordance with the theory, the surface torque was found to reach an equilibrium value after a few characteristic times $\tau_{bulk}$. During this time-interval, the surface rotation $\varphi_s - \varphi_e$ was always proportional to the instantaneous surface torque, in agreement with the predictions of equation (3) for $\xi_\gamma = 0$. Thus, these measurements demonstrate that the surface rotation is not appreciably delayed with respect to the applied surface torque. For larger times ($t \gg 6\tau_{bulk}$), the surface elastic torque remained constant with time, whilst the surface director azimuthal angle showed a very slow continuous drift.

These experimental results clearly indicate that the slow drift of the surface director angle is due mainly to a gliding of the easy axis toward the applied external field, although recent experimental results [4] demonstrate that a slow time variation of the anchoring energy coefficient also occurs—$W_a$ and $\varphi_e$ are time functions in equation (3). The gliding of the easy axis is usually explained in terms of an anisotropic adsorption–desorption of nematic molecules at the interfaces [12, 14, 15] although, in the case of polymeric substrates, a reorientation of polymeric segments could also play some role [13]. This regime is very general and has always been observed in both weak and moderately strong anchoring substrates. However, it has to be emphasized that, at the present time, no theoretical model can give a detailed description of all the experimental results.

Very recently [16], using a new high accuracy reflectometric method, we have investigated the azimuthal anchoring at the interface between a rubbed polyimide layer and the NLC 5CB. It was found that rubbed polyimide has a strong azimuthal anchoring energy ($W_a = 0.33 \times 10^{-3}\,J\,m^{-2}$ at $T = 25^\circ C$) and exhibits the characteristic slow dynamics related to director gliding. A similar gliding at a different polyimide interface has also been observed very recently by Janossy [17] using a new high accuracy optical experimental method. Due to the small amplitude of the measured surface rotations and to the very long characteristic times, our previous measurements of the director gliding at the polyimide–nematic interface were appreciably affected by thermal drift. Therefore no detailed analysis of the gliding signals was possible. In this paper, we develop a new reflectometric method where the thermal drift effects are appreciably reduced. The method allows us to obtain more accurate gliding signals and to investigate their time dependence. It is shown that the director gliding is well represented by a stretched exponential as well as for the case of weak anchoring substrates. We note that a gliding of the zenithal director angle has also been recently observed by Joly *et al.* [18] on the same polyimide used here. In this case, the gliding was also satisfactorily described by a stretched exponential. All these experimental results demonstrate that the gliding of the director is not a special feature of weak anchoring but is a very general phenomenon which involves any kind of substrate. In § 2 we describe the experimental method and the experimental apparatus. In § 3 we show the experimental results. Section 4 is devoted to conclusions.

## 2. Experimental method

Figures 1 (*a*) and 1 (*b*) show the main features of the reflectometric experimental method and of the wedge cell containing the NLC. A circularly polarized laser beam passes through a polarizer $P_1$ and impinges at a nearly normal incidence (incidence angle lower than 1°) on a NLC sandwiched between two solid plates. The solid plates are separated by two parallel thin brass electrodes $E_1$ and $E_2$ having thickness 50 and 100 μm, respectively, to make a wedge cell. The distance between the electrodes is $D = 1.78\,mm$. The NLC is inserted by capillary action into the free space between the electrodes, under vacuum in order to avoid the formation of air bubbles. The easy

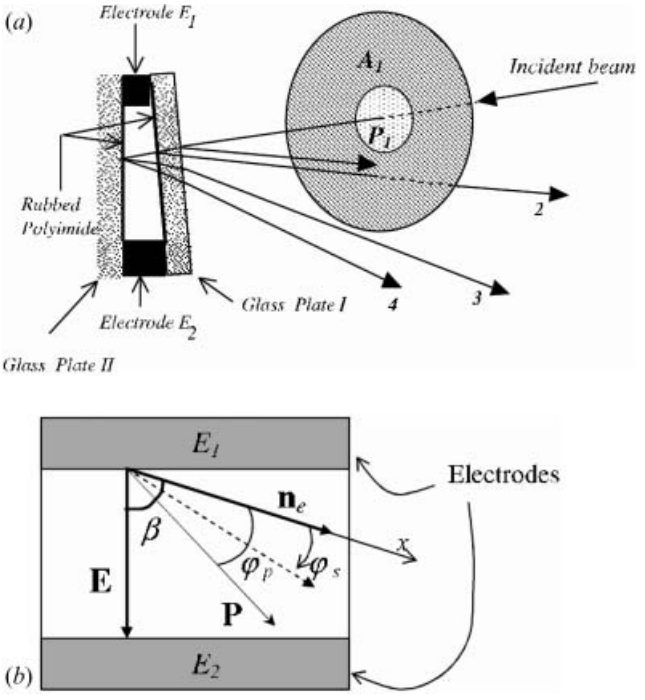


Figure 1. (*a*) Schematic view of the experimental method and of the wedge nematic cell. The two concentric circles represent polarizer $P_1$ (central circle) and analyser $A_1$ (external circle). They are two crossed polaroids glued together along the contact line. 1 and 2 are the beams reflected by the first bounding plate of the wedge nematic cell. $E_1$ and $E_2$ are parallel brass electrodes having thickness 50 µm and 100 µm, respectively. $D=1.78$ mm is the distance between the brass strips. (*b*) Top view of the cell. $\mathbf{n}_e$ is the easy axis that is assumed to be parallel to the *x* axis. **E** is the electric field and **P** is the polarizer axis of polarizer $P_1$.

axis of the director at the surface makes the azimuthal angle $\varphi_e=0$ with an *x*-axis in the plane of the substrate. An a.c. voltage $V$ is applied between the brass strips to generate a planar electric field at an angle $\beta=85^\circ$ with the *x*-axis. Under these conditions, a twist of the director field is present at the equilibrium in an interfacial layer of a few electric coherence lengths $\xi$ [1]. Due to the wedge shape of the cell, the beams reflected by the first solid plate—optical rays 1 and 2 in figure 1 (*a*)—are spatially separated from those reflected at the second plate (rays 3,4). The beams reflected by the first solid plate pass through an analyser $A_1$ which is attached to polarizer $P_1$ and crossed with respect to it. Beam 1 that is reflected by the isotropic air–glass interface has the same polarization of the incident beam and, thus, it is extinguished by the crossed analyser. The intensity of the reflected beam (optical ray 2 in the figure) after the crossed analyzer $A_1$ is [19]:

$$I = I_o c_o \left[ d_o - \cos 4\left( \varphi_p - \varphi_s - \varphi_{app} \right) \right] \qquad (4)$$

where $I_o$ is the intensity of the incident beam, $c_o$ is a suitable coefficient which depends mainly on the anisotropy of the refractive indices of the NLC, $d_o$ is a dimensionless coefficient ($d_o \cong 1$), $\varphi_p$ is the azimuthal angle of the polarizer $P_1$; $\varphi_{app}$ is a spurious contribution due to the presence of the interfacial twist and is approximately proportional to the square power of the electric field and virtually vanishes if the electric field is perpendicular to the easy axis ($\beta=90^\circ$) [19]. In our experiment we use $\beta=85^\circ$ and the maximum value of $\varphi_{app}$ (at the maximum electric field $E \approx 0.3\,\mathrm{V\,\mu m^{-1}}$) is lower than $0.01^\circ$. Therefore $\varphi_{app}$ can be disregarded and equation (4) reduces to:

$$I = I_o c_o \left[ d_o - \cos 4\left( \varphi_p - \varphi_s \right) \right]. \qquad (5)$$

In the experiment discussed in [16], the system was made by polarizer $P_1$ and analyser $A_1$ rotated with the angular velocity $\omega$. Thus, $\varphi_p$ is a linear function of time, and intensity $I$ in equation (5) becomes a sinusoidal function of time with pulsation $4\omega$ and with a phase which is simply related to the surface azimuthal angle $\varphi_s$. Therefore, $\varphi_s$ can be obtained by measuring the phase of the oscillating intensity signal. This experimental method is very direct and accurate and needs no calibration procedure. However, a time drift of the experimental signal of the order of $0.1^\circ\,h^{-1}$ is always observed. There are many possible sources for this drift, but the most important one seems to be the non-ideality of the crossed polarizers $P_1$ and $A_1$. Indeed, due to the geometrical features of our apparatus, polarizers $P_1$ and $A_1$ must be made using polaroid sheets. These materials ensure satisfactory extinction ratios ($>10^4$) only in small regions of a few millimetres, but always show appreciable variations of the extinction ratios in larger regions. Furthermore, the local extinction ratios are also functions of the temperature of the laboratory. During the rotation of the system of polarizers $P_1$–$A_1$, the reflected laser beam impinges in different regions of the analyser, see figure 1 (*a*), and, a spurious time-modulation of the transmitted beam occurs, affecting the measured phase of the reflected intensity. This spurious contribution is unimportant if one is interested in the measurement of the anchoring energy, but it appreciably affects the measurements of the gliding of the easy axis. Indeed, temperature variations occurring in the laboratory or small deflections of the laser beam lead to a slow drift of the measured phase that is superimposed on the gliding signal.

According to this discussion, the phase drift due to the polarizers could be appreciably reduced if the reflected beam always impinged the same small area (a few $mm^2$) of analyser $A_1$. Indeed it is always possible

to choose small areas of the analyser having a sufficiently high homogeneity and an extinction coefficient greater than $10^4$. This goal can be achieved by replacing the continuous rotation of polarizer $P_1$ with the oscillation

$$\varphi_p(t) = \varphi_o + a\sin(\omega t) \tag{6}$$

where $a$ is a small oscillation amplitude ($a \ll 1$ rad). Substituting $\varphi_p(t)$ of equation (6) into (5) we see that $I(t)$ becomes a periodic function of time with period $T = 2\pi/\omega$. Making a Taylor expansion of $I(\varphi_p)$ around $\varphi_p = \varphi_o$, we find that the first harmonic contribution is:

$$I_\omega(t) = 16 I_o c_o a(\varphi_o - \varphi_s)\sin(\omega t). \tag{7}$$

If the electric field is switched on, a variation $\Delta\varphi_s$ of the surface director azimuthal angle occurs, inducing the variation of the amplitude of the first harmonic component:

$$\Delta A = k\Delta\varphi_s \tag{8}$$

where $k = -16 I_o c_o a$ is a coefficient that depends on the temperature. Then, the surface director rotation $\Delta\varphi_s$ can be obtained from the measurement of $\Delta A$ if coefficient $k$ is known. Coefficient $k$ is obtained by rotating the nematic cell by a known quantity $\Delta\varphi$ and measuring the consequent amplitude variation $\Delta A$.

The experimental apparatus is shown schematically in figure 2. A He-Ne laser beam passes through a polarizer P, a tilting compensator C and is reflected by mirror $M_1$. Polarizer P and compensator C are adjusted in such a way as to compensate the anisotropy of reflection coefficients of mirror $M_1$ and to produce a circularly polarized beam after $M_1$. Then, the laser beam passes through polarizer $P_1$ and impinges on the wedge nematic cell which is inserted in a thermostated box ensuring a temperature stability better than 0.1°C. The system comprising polarizer $P_1$ and analyzer $A_1$ is connected mechanically to a high power subwoofer (300 $W_{rms}$) that oscillates at the frequency $v_o = 18$ Hz. The beams reflected by the first glass plate of the wedge cell (1 and 2 in figure 1) pass through the crossed analyser $A_1$ and are focused on photodiode $Ph_1$. A small portion of the beam which passes through polarizer $P_1$ is reflected at nearly normal incidence by a glass wedge plate ($W$ in figure 2), passes through an analyser ($P_2$) and is focused on photodiode $Ph_2$. When polarizer $P_1$ is oscillating and $P_2$ is set close to the extinction position, the output $I_2$ of photodiode $Ph_2$ is a periodic function of period $2\pi/\omega$ with a first harmonic proportional to the average angle between the axes of the two polarizers and to the polarizer oscillation amplitude $a$. This latter signal permits the control of any drift of the oscillation amplitude $a$, of the average azimuthal angle $\varphi_o$ of polarizer $P_1$ and of the laser intensity. Photodiode outputs $I_1$ and $I_2$ of are sent to the inputs of two lock-in amplifiers and the outputs of the lock-in amplifiers are sent to a PC.

## 3. Experimental results

An a.c. voltage (up to 700 $V_{rms}$) of frequency $v = 500$ Hz can be applied between the two electrodes of the cell. The wave period is smaller than the relaxation time of ionic charges and than the minimum director response time. In these conditions, the oscillating electric field is equivalent to a d.c. electric field having an intensity equal to its rms value [1]. The maximum electric field

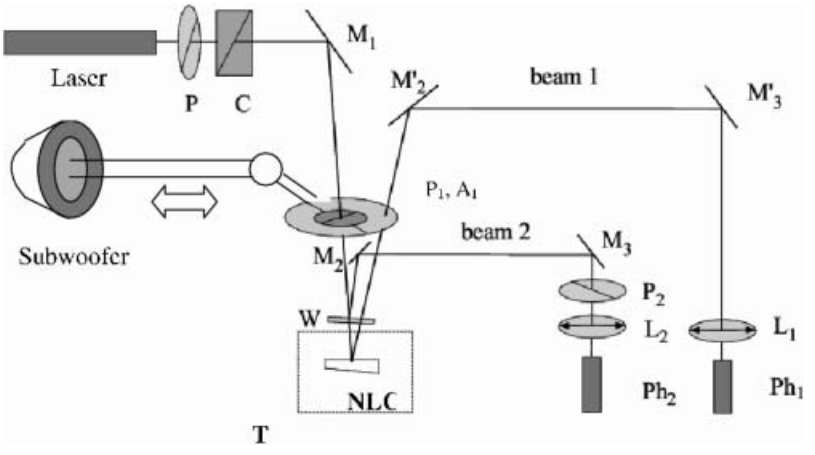


Figure 2. Schematic view of the experimental apparatus. P,$P_1$,$P_2$=polarizers; C=tilting optical compensator; $A_1$=crossed analyser; $M_1$,$M_2$,$M_3$,$M'_2$,$M'_3$=mirrors; $L_1$,$L_2$=lenses; $Ph_1$,$Ph_2$=photodiodes; W=glass wedge plate; T=termostatic box; NLC=wedge cell containing the nematic liquid crystal.

torque is equivalent to the torque produced by a magnetic induction $B \approx 4\,\mathrm{T}$. In order to reduce the electric field gradients that characterize this type of planar electric field, the electric voltage was obtained using a special voltage amplifier giving two outputs, $V_1 = V/2$ and $V_2 = -V/2$, that are symmetrical with respect to ground. These two outputs were connected to the two brass electrodes of the nematic cell. Using a special experimental procedure [16, 20] we measured the space dependence of the electric field in the region between the two electrodes. The electric field increases close to the electrodes but is virtually uniform in a central stripe of width 0.6 mm between them. In this central region, the rms value $E$ of the electric field is $E = 0.90\,V/D$, where $V$ is the rms value of the oscillating voltage and $D = 1.78\,\mathrm{mm}$ is the distance between the electrodes. To avoid any spurious effect due to electric field gradients, our measurements were performed by focusing the laser beam (beam waist $\approx 0.25\,\mathrm{mm}$) in the central region between the electrodes where the electric field is virtually uniform.

The NLC is 4-pentyl-4′-cianobiphenyl (5CB) purchased from Merck, having a clearing temperature $T_c = 35^\circ\mathrm{C}$. The two internal surfaces of the glass plates in figures 1 (*a*) and 1 (*b*) are covered by a thin polyimide layer (Nissan Corporation SE-3510), rubbed using a velvet roll along a given axis in the plane of the layer. The rubbing is unidirectional and performed once (one passage). This kind of interface leads to an easy axis aligned along the rubbing direction with pretilt angle $\theta_p \approx 6^\circ$. The rubbed polyimide glass plates were kindly supplied by S. Joly of Nemoptic. Using the definition of rubbing strength $L$ given in equation (2) of [21], we find $L = 5\,\mathrm{m}$ that corresponds to a high rubbing strength.

In our experiment, the a.c. electric field is switched on at a given time $t$ and the consequent amplitude variation $\Delta A$ of the first harmonic is measured. Substituting $\Delta A$ together with the experimental value of coefficient $k$ in equation (8), we obtain the time variation $\Delta\varphi_s$ of the surface azimuthal angle. After a short time interval ($\cong 6\tau_{bulk}$), $\Delta\varphi_s$ reaches a near–equilibrium value $\Delta\varphi_s$(n.e.) that is related to the azimuthal anchoring energy coefficient $W_a$ by the simple relation:

$$\Delta\phi_s(\mathrm{n.e.}) = \frac{(K_{22}\varepsilon_a\varepsilon_o)^{\frac{1}{2}}\sin\beta}{W_a}E \qquad (9)$$

where $K_{22}$ is the twist elastic constant of 5CB [22]. Equation (9) holds if the electric field is much higher than the Fréederickz threshold field $E_c$ [1] ($E_c < 0.01\,\mathrm{V\,\mu m^{-1}}$ in our experiment) and if $\Delta\varphi_s(\mathrm{n.e.}) \ll 1\,\mathrm{rad}$.

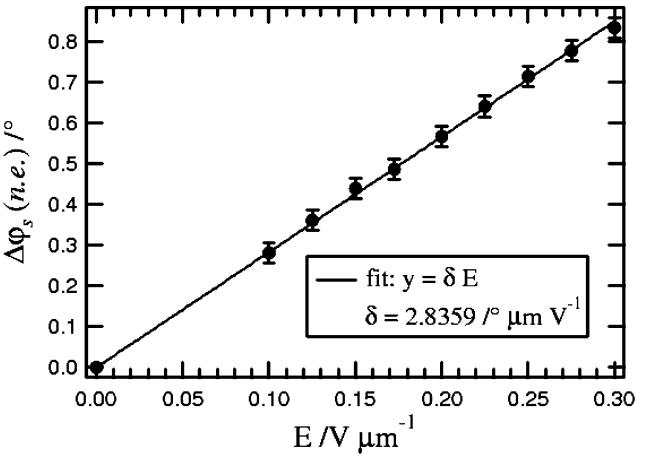


Figure 3. Near-equilibrium variation $\Delta\varphi_s$(n.e.) of the azimuthal angle versus the rms electric field. Points correspond to the experimental values, the full line corresponds to the best fit with function $y = \delta\mathbf{E}$. The sample temperature is $T = 25.1^\circ\mathrm{C}$. The electric field is applied at angle $\beta = 85^\circ$ with respect to the easy axis. The error bars in the figure correspond to two standard deviations.

The points in figure 3 show the measured near-equilibrium values of $\Delta\varphi_s$ versus the rms value of the applied electric field. The temperature of the NLC is 25.1°C. The line in figure 3 represents the best fit with the linear function $\Delta\varphi_s(\mathrm{n.e.}) = \delta\ E$ where $\delta$ is a free parameter. The azimuthal anchoring energy coefficient $W_a$ is obtained by substituting in equation (9) $K_{22} = 3.93 \times 10^{-12}\,\mathrm{N}$ [22], $\varepsilon_a = 13.1$ [7] and the best fit coefficient $\delta = 2.836^\circ\,\mu\mathrm{m\,V^{-1}} = 4.95 \times 10^{-2}\,\mathrm{rad\,\mu m\,V^{-1}}$. We find $W_a = 0.43 \times 10^{-3}\,\mathrm{J\,m^{-2}}$, which is comparable but slightly higher than the value $W_a = 0.33 \times 10^{-3}\,\mathrm{J\,m^{-2}}$ that we measured on the same substrate and at the same temperature using the rotating polarizer method [16]. The corresponding extrapolation length [1, 2] is $d_e = K_{22}/W_a = 9.1\,\mathrm{nm}$. Therefore, this measurement also confirms that the azimuthal anchoring at the rubbed polyimide interface is strong.

These high azimuthal anchoring values are also comparable to the values measured by one of us [23] and by Janossy [17] using high accuracy transmission light methods on a different polyimide sample. On the other hand, it has to be noted that these values of the anchoring energy are much higher than the experimental values reported in the literature for rubbed polymer–nematic interfaces [24–26]. Unfortunately, the value of the rubbing strength $L$ was not reported in these references, therefore it is not possible to make a full comparison with our experimental results. In fact, for the interface between a nematic liquid crystal and a PVA polymer, Sato *et al.* [21] showed that the extrapolation length $d_e$ at a polymer–nematic interface

is inversely proportional to the rubbing strength $L$. At the maximum value of $L$ ($L=0.9$ m) they found $d_e=80$ nm. In our experiment, the rubbing strength is somewhat higher ($L=5$ m). Therefore, it is possible that the different values of the azimuthal anchoring energies measured here and in other experiments can be justified by very different rubbing strengths.

However, it must also be emphasized that the transmission light methods that are currently used in the literature to measure the azimuthal anchoring energy need very special care to avoid spurious contributions due to the bulk director distortion. As shown in detail in ref. [27], these spurious contributions can simulate the occurrence of a weak anchoring energy also in the case of substrates characterized by a very strong anchoring. By contrast, the reflectometric methods used here and in [16] are virtually unaffected by the bulk director distortion. Furthermore, in the case of the rotating polarizers method [19], the surface rotation angle $\Delta\varphi_s$ is proportional to the measured phase change $\Delta\Phi$ of the oscillating intensity ($\Delta\varphi_s=\Delta\Phi/4$). Then, the reflectometric measurement of the surface director rotation is very direct and requires no calibration procedure or any knowledge of the material parameters of the nematic liquid crystals. For a detailed discussion of the reflectometric method and its advantages with respect to the transmitted light methods, see [19].

It must be emphasized that the experimental method developed here, although less affected by thermal drift, provides less accurate experimental measurements of the azimuthal anchoring energy with respect to the rotating polarizer method used in [16]. This lower accuracy is demonstrated by a lower repeatability of the measurements of azimuthal anchoring energy. Furthermore, the anchoring energies measured at $T=25^\circ$C at different points of the cell showed appreciable variations (up to $\pm 40\%$ with respect to an average value $W_a \approx 0.32\times10^{-3}$ J m$^{-2}$). These space variations were not found using the rotating polarizer method.

As previously shown [16], the azimuthal anchoring energy is a decreasing function of the temperature of the sample. For this reason, in order to obtain larger experimental signals and reduced relative drifts, the director gliding has been investigated at a temperature appreciably higher than the room temperature. Figure 4 (*a*) shows the time-variation of the surface director azimuthal angle when the electric field is switched on. The applied electric field is $E=0.25$ V μm$^{-1}$ and the temperature is $T=32.7^\circ$C. The electric field is switched on at time $t=0$ min. Figure 4 (*b*) shows a detail of the time response at the switching on time. An analogous slow reorientation is observed at the switching off of the electric field. The broken lines in figures 4 (*a*) and 4 (*b*) represent the theoretical behaviour that would be predicted by the classical theory of the anchoring in the absence of director gliding, and by accounting for the lock-in integration time. It is evident from figures 4 (*a*) and 4 (*b*) that two very different time regimes occur: a first short time regime and a successive gliding regime characterized by very long relaxation times. During the first regime, the surface director follows the bulk reorientation of the director field and reaches an almost equilibrium value $\Delta\varphi_s$(n.e.)$=1.4^\circ$ after a few characteristic bulk times. In the case of the

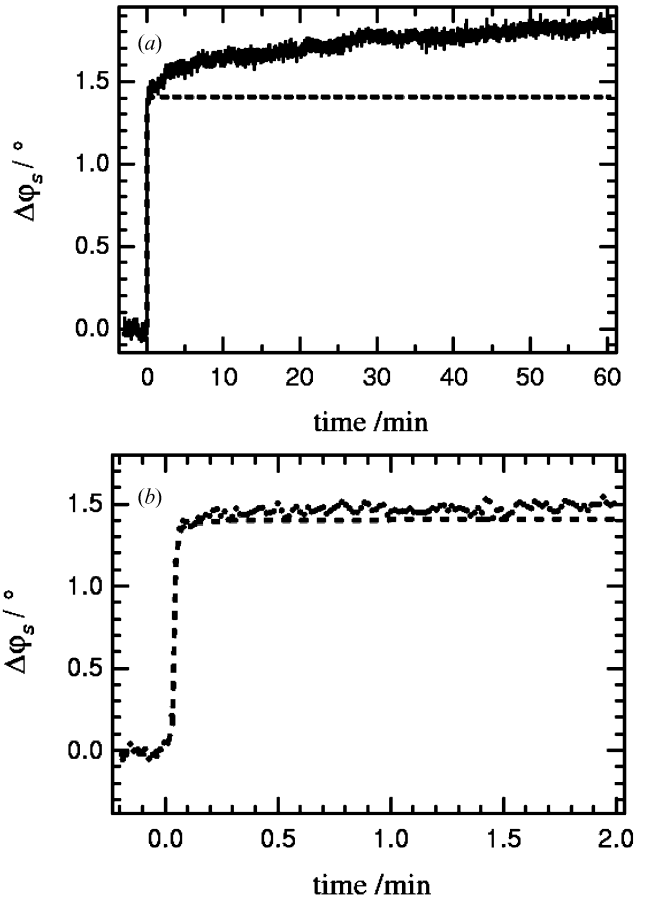


Figure 4. (*a*) Time variation $\Delta\varphi_s(t)$ of the surface azimuthal angle at the switching on of the electric field $E=0.25$ V μm$^{-1}$rms. The electric field is switched on at time $t=0$ min; the temperature of the nematic sample is 32.7°C. The broken line represents the theoretical response predicted by the continuum theory in the absence of gliding of the easy axis and by taking into account the integration time of the lock-in (integration time $\tau=0.3$ s with a 12 dB filter). After some integration times, the broken line reaches the near-equilibrium value $\Delta\varphi_s$(n.e.)$=1.4^\circ$. (*b*) A detail of the experimental results shown in (*a*) close to the switching on time $t=0$. The broken line corresponds to the theoretically predicted behaviour in the absence of gliding.

experiment shown in figure 4 (*a*), the electric field is $E=0.25\,\mathrm{V\,\mu m^{-1}}$ and the bulk relaxation time [$\tau_{bulk}=\gamma/(\varepsilon_a\,\varepsilon_o\,E^2)$] is $\tau_{bulk}\approx 11$ ms, which is much smaller than the lock-in response time (time constant $\tau_o=0.3$ s of a 12 dB filter). Therefore, the first short response in figures 4 (*a*) and 4 (*b*) is dominated by the lock-in response time. The true bulk reorientation can be observed only for smaller electric fields where $\tau_{bulk}$ becomes greater than the lock-in response time. The gliding regime is characterized by much longer characteristic times.

Figure 5 shows the experimental values of the gliding rotation angle $\Delta\phi_s^*(t)=\Delta\varphi_s(t)-\Delta\varphi_s(\mathrm{n.e.})$ which is obtained by subtracting the near-equilibrium value from the experimental values of $\Delta\varphi_s(t)$ shown in figure 4 (*a*). Only the experimental points obtained after the response time of the lock-in filter ($6\tau_o\approx 2$ s) are shown in figure 5. Furthermore, to make the figure clearer, a smoothing procedure has been applied to the experimental data. Of course, the gliding rotation angle $\Delta\phi_s^*(t)$ vanishes at $t=0$. The broken line corresponds to the best fit of the experimental results with the single exponential function $y=a_o\,[1-\exp(-t/\tau)]$, where $a_o$ and $\tau$ are free fitting parameters ($a_o=0.377^\circ$ and $\tau=14.2$ min). It is evident that this time dependence does not correctly reproduce the experimental behaviour and, in particular, the long time behaviour. In fact, the gliding signal is characterized by at least two different characteristic.

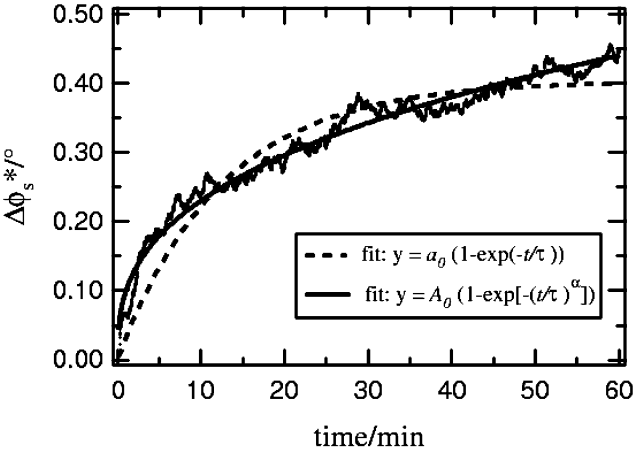


Figure 5. Gliding contribution $\Delta\phi_s^*(t)=\Delta\varphi_s(t)-\Delta\varphi_s(\mathrm{n.e.})$ versus time. The values of $\Delta\phi_s^*(t)$ are obtained from the data in figure 4 (*a*) using a smoothing procedure to clarify the comparison with the theoretical fit curves. The broken and full lines correspond to the best fits with the single exponential function $y=a_o[1-\exp(-t/\tau)]$ and with the stretched exponential function $y=A_o[1-\exp(-(t/\tau)^\alpha)]$, respectively. Both these functions have only two free parameters ($a_o$, $\tau$ and $\tau$, $\alpha$, respectively). Parameter $A_o$ in the stretched exponential is fixed to $A_o=\beta-\Delta\varphi_s$ (n.e.)$=83.6^\circ$ by the physical condition that the surface director tends to align along the electric field.

According to the proposed models of gliding [13, 15, 18] and to some experimental results with weak anchoring [4], one expects that the easy axis tends to align along the electric field, which initially forms angle $\beta=85^\circ$ with respect to the initial orientation of the easy axis. Then, $\Delta\phi_s^*(t)=\Delta\varphi_s(t)-\Delta\varphi_s(\mathrm{n.e.})$ tends to $A_o=\beta-\Delta\varphi_s$ (n.e.)$=83.6^\circ$ for $t\to\infty$. Furthermore, according to the previous experimental results, we expect that the time dependence of the gliding is well represented by a stretched exponential [4, 14, 18] or a power law function [13]. Here, we compare our experimental results with the stretched exponential function:

$$\Delta\phi_s^*(t)=A_o[1-\exp(-(t/\tau)^\alpha)] \qquad (10)$$

where $A_o=83.6^\circ$ is a fixed parameter, whilst $\tau$ and $\alpha$ are the only two fitting free parameters. Such a function automatically satisfies both the limit conditions $\Delta\phi_s^*(0)=0$ and $\Delta\phi_s^*(t)\to A_0$ for $t\to\infty$. The full line in figure 5 shows the best fit curve corresponding to the best fit parameters $\tau=1.16\times 10^8$ min and $\alpha=0.362$. We note that $\tau$ is much greater than the measurement time (60 min in our experiment); then, in this time interval, the stretched exponential in equation (10) can be suitably replaced by its power expansion in the small parameter $t'=(t/\tau)^\alpha$ stopped at the first significant contribution that is $\Delta\phi_s^*(t')=A_0t'+\ldots..$ This means that the stretched exponential is indistinguishable from the power law $y=A\,t^\gamma$, provided that $A=A_o/\tau^\alpha$ and $\gamma=\alpha$. By taking into account the experimental noise and the fact that there are only two free fitting parameters, the agreement between the experimental results and the stretched exponential is satisfactory.

We note that, in our case, the study of the gliding signal has been restricted to an hour time due to the presence of some residual drift. In such a case, a fit with a two-exponential function with the only limit condition $\Delta\phi_s^*(0)=0$ and with four free parameters leads to a slightly better agreement with the experimental results. However, according to the experimental results obtained in the case of weak anchoring substrates [4] and for the zenithal anchoring at the same polyimide interface [18] we think that this agreement should disappear if a longer time interval wese investigated.

## 4. Concluding remarks

In this paper we describe the development of a new reflectometric method to measure the surface director azimuthal angle at a NLC interface. Besides the rotating polarizer technique, this method needs a calibration procedure that makes it less efficient and accurate for measurements of anchoring energy. However, the method is affected by smaller thermal drifts and, thus,

it is more useful to measure the director gliding. The long time behaviour of the surface director azimuthal angle has been investigated at the rubbed polyimide–5CB interface. Although appreciable noise is still present in our measurements, it has been possible to obtain sufficiently accurate gliding signals. It has been shown that the dynamics at this type of interface shows the same characteristic features that have already been observed in the case of weakly anchored interfaces. In particular, the gliding signal is non-exponential and can be reproduced satisfactorily by a stretched exponential function with only two free fitting parameters, as in the case of weak anchoring. This latter function, together with power laws, is usually used to describe the dynamic behaviour of physical systems that are characterized by a multiplicity of relaxation times as well as, for instance, glasses and polymers (see, for example, the interesting review paper [28]). It is important to emphasize that a gliding of the zenithal surface director angle with similar qualitative features has also been recently observed on the same interface [18].

Our experimental results, together with those reported in [17, 18], demonstrate that the gliding phenomenon is not restricted to the special case of weak anchoring and of azimuthal anchoring but is a very general phenomenon that characterizes the surface interactions of nematic liquid crystals. In fact, to date we have always observed the gliding phenomenon for any type of interface investigated—glass, SiO, PVA, polyimide, teflon, photosensitive polymers, etc. Therefore, we hope that these experimental results can stimulate further interest in this important aspect of the surface physics of NLCs. Indeed, at the present time, the proposed models of the director gliding are somewhat rough and are unable to explain satisfactorily all the quantitative and qualitative features of the experimental results.



## Acknowledgements

We acknowledge Dr S. Joly and Dr I. Dozov of Nemoptic for suggesting this experiment to us and for supplying the rubbed polyimide glasses.

## References

[1] P.G. de Gennes. *The Physics of Liquid Crystals*. Clarendon Press, Oxford (1974).
[2] S. Faetti. *Physics of Liquid Crystalline Materials*, I.C. Khoo, F. Simoni (Eds). Gordon and Breach (1991).
[3] M. Nobili, C. Lazzari, A. Schirone, S. Faetti. *Mol. Cryst. liq. Cryst.*, **212**, 97 (1992).
[4] I. Gerus, S. Faetti, G.C. Mutinati. *Mol. Cryst. liq. Cryst.*, **421**, 81 (2004).
[5] A. Mertelj, M. Copic. *Phys. Rev. Lett.*, **81**, 5844 (1998).
[6] H.J. Coles, M.S. Sefton. *Mol. Cryst. liq. Cryst. Lett.*, **3**, 63 (1976).
[7] A. Bogi, S. Faetti. *Liq. Cryst.*, **28**, 729 (2001).
[8] R. Barberi, I. Dozov, M. Giocondo, M. Iovane, P. Martinot Lagarde, D. Stoenescu, S. Tonchev, L.V. Tsonev. *Eur. Phys. J. B*, **6**, 83 (1998).
[9] E.A. Olivera, A.M. Figueredo Neto, G. Durand. *Phys. Rev. A*, **44**, R825 (1991).
[10] T. Nose, S. Masuda, S. Sato. *Jpn. J. appl. Phys.*, **30**, 3450 (1991).
[11] P. Vetter, Y. Ohmura, T. Uchida. *Jpn. J. appl. Phys. 2*, **32**, L-1239 (1955).
[12] V.P. Vorflusev, H.S. Kitzerow, V.G. Chigrinov. *Appl. Phys. Lett.*, **70**, 3359 (1997).
[13] I. Janossy, T.I. Kosa. *Phys. Rev. E*, **70**, 052701 (2004).
[14] S. Faetti, M. Nobili, I. Raggi. *Eur. Phys. J. B*, **11**, 445 (1999).
[15] A. Romanenko, I. Pinkevich, V. Reshetnyak, I. Dozov, D. Stoenescu. *Mol. Cryst. liq. Cryst.*, **422**, 173 (2004).
[16] S. Faetti, P. Marianelli, *Phys. Rev. E*, **72**, 051708 (2005).
[17] I. Janossy, *J. Appl. Phys.*, **98**, 043523 (2005).
[18] S. Joly, K. Antonova, P. Martinot Lagarde, I. Dozov. *Phys. Rev. E*, **70**, 050701R (2004).
[19] S. Faetti, G.C. Mutinati. *Eur, Phys. J. E*, **10**, 265 (2003).
[20] P. Marianelli. PhD thesis, University of Pisa, Italy (2005).
[21] Y. Sato, K. Sato, T. Uchida. *Jpn. J. appl. Phys. 2*, **31**, L579 (1992).
[22] T. Toyooka, G. Chen, H. Takezoe, A. Fukuda. *Jpn. J. appl. Phys.*, **26**, 1959 (1987).
[23] S. Faetti. *Mol. Cryst. liq. Cryst.*, **421**, 225 (2004).
[24] T.Oh. Ide, S. Kuniyasu, S. Kobayashi. *Mol. Cryst. liq. Cryst.*, **164**, 91 (1988).
[25] M. Vilfan, M. Copic. *Phys. Rev. E 1*, **68**, 031704 (2003).
[26] B. Zhang, P. Sheng, H.S. Kwok. *Phys. Rev. E 1*, **67**, 041713 (2003).
[27] S. Faetti, G.C. Mutinati. *Phys. Rev. E., 2*, **68**, 026601 (2003).
[28] C.A. Angell, K.L. Ngai, G.B. McKenna, P.F. McMillan, S.W. Martin. *J. appl. Phys.*, **88**, 3113 (2000).